Does Thin Filament Compliance Diminish the Cross-Bridge Kinetics? A Study in Rabbit Psoas Fibers

Gang Wang, Wei Ding, and Masataka Kawai

Department of Anatomy and Cell Biology, College of Medicine, The University of Iowa, Iowa City, IA 52242, USA

ABSTRACT   The effect of thin filament compliance on our ability to detect the cross-bridge kinetics was examined. Our experiment is based on the facts that in rabbit psoas the thin filament (1.12 μm) is longer than half the thick filament length (0.82 μm) and that the thick filament has a central bare zone (0.16 μm). Consequently, when sarcomere length is increased from 2.1 to 2.4 μm, the same number of cross-bridges is involved in force generation but extra series compliance is introduced in the I-band. Three apparent rate constants (2πa, 2πb, and 2πc) were characterized by sinusoidal analysis at pCa 4.66. Our results demonstrate that 2πa and 2πb increased 13–16% when sarcomere length was increased from 2.0 to 2.5 μm, and 2πc decreased slightly (9%). This slight decrease can be explained by compression of the lattice spacing. These observations are at variance with the expectation based on increased series compliance, which predicts that the rate constants will decrease. We also determined compliance of the I-band during rigor. I-band compliance during rigor induction was 35% of sarcomere compliance at sarcomere length 2.4 μm, and 24% at sarcomere length 2.1 μm. We conclude that the presence of thin filament compliance does not seriously interfere with our ability to detect cross-bridge kinetics using sinusoidal analysis.

INTRODUCTION

It has long been assumed for the sake of simplicity that the thick and thin filaments are rigid and the length change applied to a sarcomere is directly applied to cross-bridges (A. F. Huxley, 1957; A. F. Huxley and Simmons, 1971). However, this view has been challenged in recent years by meridional x-ray diffraction studies on intact, tetanically stimulated sartorius and semitendinosus muscles of the bullfrog (Wakabayashi et al., 1994; H. E. Huxley et al., 1994) and by stiffness measurements at different sarcomere lengths in frog semitendinosus (Bagni et al., 1990), frog tibialis anterior (Linari et al., 1998), and rabbit psoas (Higuchi et al., 1995) fibers. One of these reports estimated that the compliance of the thin filament is 42% of the total sarcomere compliance; of the thick filament, 27%; and of the cross-bridges, 31% (Wakabayashi et al., 1994). The other estimate of the thin filaments ranged from 19% (Bagni et al., 1990) to 44% (Higuchi et al., 1995), based on mechanical measurements. Thus, because of the high series compliance of the filaments, it is essential to know the effect of that compliance on the time course of tension transients or, more specifically, on the measured rate constants. The tension transients can be induced in the steady state by a perturbation such as length change (e.g., A. F. Huxley and Simmons, 1971; Kawai and Brandt, 1980), temperature increase (e.g., Ranatunga, 1996), pressure release (e.g., Fortune et al., 1991), or an increase in the ligand concentration (e.g., Dantzig et al., 1992). In these cases, the perturbation

must be faster than the process being measured so that the time course reflects the process and not the perturbation.

Two general methods to resolve the problem of in-series compliance are a theoretical approach and an experimental approach. Luo et al. (1993) used a theoretical approach, which put a series compliance in A. F. Huxley's (1957) model, the simplified mechanical equivalent of which is shown in Fig. 1, for the purpose of perturbation analysis. Here an exponential process (or cross-bridge response) is represented by a spring and a dashpot linked in series. The apparent rate constant r of this exponential process is determined by the spring constant (k) and viscosity of the dashpot (η), and $r = k/\eta$. If a series compliance (q) is added, this diminishes the rate constant r according to Eq. 1:

$$r = \frac{1}{\eta(1/k + q)} = \frac{k}{\eta(1 + kq)} \qquad (1)$$

$q = 0$ represents the case in which no series compliance is involved. If cross-bridge stiffness (k) is comparable to the stiffness ($1/q$) of the series compliance as reported (Wakabayashi et al., 1994), then $kq \sim 1$. Thus, from Eq. 1, a 50% reduction in the apparent rate constant is expected if series filament stiffness is comparable to that of the cross-bridges. Luo et al. (1993) similarly predicted a reduction of the apparent rate constant.

In this report, we chose an experimental approach and studied the cross-bridge kinetics as sarcomere length (SL) was altered. In particular, we aimed at comparing the kinetic constants of elementary steps at SL = 2.1 μm and SL = 2.4 μm in rabbit psoas fibers during maximal Ca^{2+} activation (pCa 4.66). At these two sarcomere lengths, the number of cross-bridges available for actin-myosin interaction is the same, whereas at SL = 2.4 μm there is an extra length of the thin filament which serves as in-series compliance in
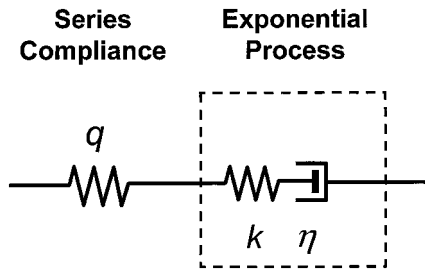
FIGURE 1   An arrangement of an exponential process and a series compliance. Here the exponential process is represented by an elastic component (k = spring constant) and a dashpot (η = viscosity), which give the composite rate constant of k/η. The series compliance is q. The apparent rate constant for this arrangement is given in Eq. 1.

rabbit psoas fibers (Higuchi et al., 1995). Because series compliance (due to the thin filament) is proportional to the width of the I-band, it has been estimated that thin filament compliance is 1.7 times greater at SL = 2.4 μm than at 2.1 μm. Based on Eq. 1, this would yield rate constants 21% slower at SL = 2.4 μm than at SL = 2.1 μm. The model of Luo et al. (1993) similarly predicts a 20–25% reduction in the apparent rate constant. Therefore, one can determine the effect of extra series compliance on the rate constants by studying them at two different sarcomere lengths. Quite interestingly, our results indicate that two rate constants, $2\pi a$ and $2\pi b$, increase, and one rate constant, $2\pi c$, decreases, but only slightly (9%), with SL, demonstrating that the rate constants do not diminish as expected. Preliminary accounts of these results have been presented (Wang and Kawai, 1997).

METHODS

Single-skinned psoas muscle fibers from the rabbit were used for this study. SL was determined by optical diffraction using a He-Ne laser (λ = 632.8 nm) during both relaxation and activation. The diameter of the preparation was determined by a compound microscope with Nomarsky optics (Leitz Diavert, 200$\times$). Experiments were performed at seven different SLs (1.7, 1.8, 2.1, 2.4, 2.7, 3.0, and 3.5 μm). The preparation was relaxed before each SL change. Fig. 2 is a plot of the fiber length against SL measured during relaxation. The fiber length was normalized to that at SL = 2.4 μm for the purpose of averaging because the length was different for each preparation. The plot in Fig. 2 demonstrates that SL is approximately proportional to the applied length change, which implies there is no extra compliance at the ends during relaxation.

When isometric tension reached a steady state, the length of the fibers was changed in sinewaves of varying frequencies (0.25–350 Hz, corresponding to 0.5–640 ms in time domain) and the tension time course was collected. The amplitude of the length change was 0.125% of L_0 (L_0 is the length of the fiber at SL = 2.4 μm), which corresponds to 1.5 nm per half sarcomere. The complex modulus $Y(f)$ is defined as the ratio of the stress change to the strain change in the frequency (f) domain and is represented by a complex number. $Y(f)$ can be resolved into three exponential processes, A, B, and C, defined in order of increasing speed.

Process A   Process B   Process C

$$Y(f) = H + A/(1 + a/fi) - B/(1 + b/fi) + C/(1 + c/fi)$$
(2)

In this equation, $i = \sqrt{-1}$. Lower case letters a, b, and c represent characteristic frequencies of exponential processes ($a < b < c$), and upper
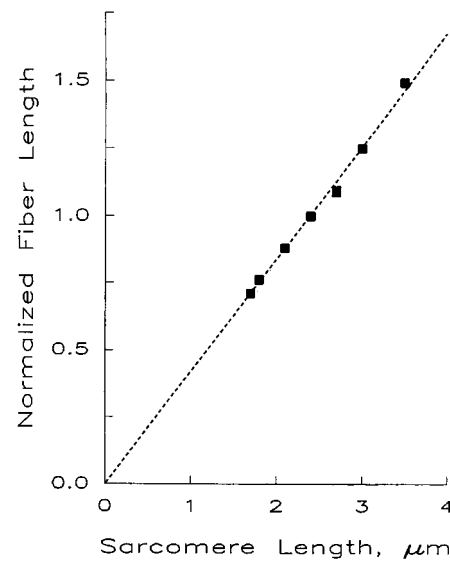

FIGURE 2   Fiber length is plotted against the sarcomere length (SL) during BDM relaxation. The fiber length was normalized to that at SL = 2.4 μm and averaged and plotted with SE error bars. Most of the error bars are smaller than the symbol size and cannot be seen. $n = 15$ (SL = 1.7–2.4 μm), $n = 6$ (2.7 μm), $n = 1$ (3.0–3.5 μm). This plot demonstrates that sarcomeres are stretched proportionally to the fiber length during BDM relaxation.

case letters A, B, and C represent their respective magnitudes. 2π times the characteristic frequencies are the apparent (measured) rate constants. H is the elastic modulus extrapolated to zero frequency. The elastic modulus extrapolated to the infinite (∞) frequency is defined as:

$$Y_\infty = H + A - B + C$$
(3)

Y_∞ corresponds to phase 1 of step analysis. Process C corresponds to phase 2, process B to phase 3, and process A to phase 4 of step analysis. Details of the sinusoidal analysis method were published previously (Kawai and Brandt, 1980).

The control-activating solution consisted of 6 mM K_2 CaEGTA, 5.8 mM Na_2MgATP, 1.4 mM $Na_2K_{1.7}ATP$, 15 mM creatine phosphate (Na_2CP), 8 mM phosphate ($Na_{1.5}K_{1.5}Pi$), 11 mM Na propionate (NaProp), 73 mM KProp, 10 mM MOPS, and 320 unit/ml creatine kinase (pCa 4.66, Mg^{2+} 0.5 mM, pH 7.0, total Na 55 mM, ionic strength 200 mM). At SL $<$ 2.4 μm, the relaxation was achieved by the same control-activating solution containing 50 mM 2,3-butanedione monoxime (BDM) (Higuchi et al., 1995). With the conventional relaxing solution containing ATP and EGTA (see below), the fiber buckles if fiber length is set for SL $<$ 2.4 μm. Thus, a weak contracting solution such as the BDM-Ca solution is essential for experiments that use short SL. As was reported earlier (Zhao and Kawai, 1994a), BDM stimulates the ATP binding step and diminishes the force generation step to help relax muscle fibers (see also Higuchi et al., 1995). At SL $\geq$ 2.4 μm, the fibers were relaxed by conventional relaxing solution that contained 6 mM EGTA, 2 mM Na_2MgATP, 5 mM $Na_2K_{1.7}ATP$, 8 mM Pi, 62 mM NaProp, 48 mM Kprop, and 10 mM MOPS (pH 7.0). The source of chemicals and other experimental details are the same as reported previously (Wang and Kawai, 1996; Zhao et al., 1996).

Rigor was induced from control activation by two washes with the rigor-2 solution containing 8 mM $K_{1.5}Pi$, 76 mM NaProp, 103 mM KProp, and 10 mM MOPS (pH adjusted to 7.0). This rigor corresponds to the "high-rigor" state reported earlier (Kawai and Brandt, 1976), where rigor tension is similar to active tension, whereas rigor stiffness is higher than active stiffness in all frequencies. The complex modulus data of the rigor fibers were collected at the end of a series of experiments and used as the reference material to correct for the system function. At each SL, both

resting and active complex moduli were measured and the resting modulus was subtracted from the active modulus before plotting the data or fitting the data to Eq. 2. The subtraction becomes significant at SL > 3.0 μm, but it is negligible at SL ≤ 3 μm. Since BDM-Ca solution was used only at SL < 2.4 μm to relax fibers, use of this solution does not affect the results at all. The above method of subtraction assumes that the elements responsible for the resting complex modulus do not change their mechanical properties during Ca^{2+} activation, and that these elements are mechanically in parallel with cross-bridges. Those contributing to the resting complex modulus are connectin-titin and residual sarcolemma. There is little evidence to date that their mechanical properties change with Ca^{2+} activation.

RESULTS

Fig. 3 summarizes the amount of sarcomere shortening during control activation. Fig. 4 summarizes the isometric tension plotted against the SL in the same control activation. Resting tension was subtracted from the plot. In Fig. 3, it is seen that sarcomere shortening was largest at SL $= 2.7$ μm, amounting to 0.2 μm. At shorter SL, the shortening was smaller and ≤ 0.1 μm. There was little shortening at SL $= 3.0$ μm and a slight elongation was noticeable at SL $= 3.5$ μm. As seen in Fig. 4, isometric tension (dotted line) increased as SL was increased from 1.7 μm to 2.4 μm. Tension was not significantly different at SL $= 2.4$ and 2.7 μm and it declined when SL was further increased to 3.5 μm. Because the SL change occurred during activation (Fig. 3), each point was shifted along the abscissa by using the averaged data in Fig. 3. The horizontal error bars in Fig. 4 are the same as those in Fig. 3. The length-tension plot is similar to that of Stephenson and Williams (1982).

Fig. 5 summarizes the width of the preparation normalized to that at SL $= 2.4$ μm during relaxation. The width, which shrank during activation, was approximately linearly correlated with SL and decreased with SL. By using equa-

FIGURE 4   Length-tension diagram. The tension value during activation was normalized to that at SL $= 2.4$ μm, averaged, and plotted with SE. There were 14 observations at SL $= 1.7$–2.1 μm, 29 at 2.4 μm, 18 at 2.7 μm, and 13 at 3.0–3.5 μm. The fibers were activated in the control-activating solution. Resting tension was subtracted from the data. The dotted line (⋯⋯) represents the data based on the SL measured during relaxation. Symbols and the solid line and squares (—■—) represent the data that considered sarcomere shortening (or elongation) during control activation and as shown in Fig. 3. Horizontal error bars are those from Fig. 3.

torial x-ray diffraction technique, it was reported that the fiber width is directly proportional to the lattice spacing of the thick and thin filaments in chemically skinned rabbit psoas fibers (Kawai et al., 1993).

Fig. 6 A plots the elastic modulus against frequency and Fig. 6 B plots the viscous modulus against frequency at three SLs (2.1, 2.4, and 2.7 μm) during control activation.
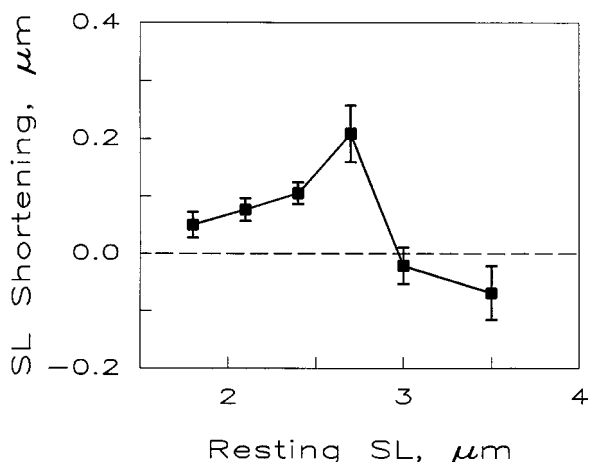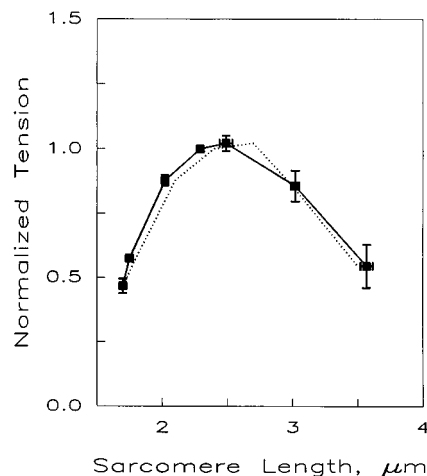

FIGURE 3   The degree of sarcomere shortening, in millimeters, in the midsection (2 mm) of fibers during control activation was measured by optical diffraction ($\lambda = 632.8$ nm), then averaged and plotted against SL with SE. There were 7 observations at SL $= 1.8$ μm, 13 at 2.1 μm, 36 at 2.4 μm, 23 at 2.7 μm, 19 at 3.0 μm, and 16 at 3.5 μm. The control-activating solution contained 6 mM CaEGTA, 5 mM MgATP^{2-}, 8 mM Pi, 15 mM CP, 10 mM MOPS, 10 mM NaProp, 82 mM Kprop, and 320 u/ml CK (0.5 Mg^{2+}, ionic strength 200, pCa 4.66, pH 7.0).
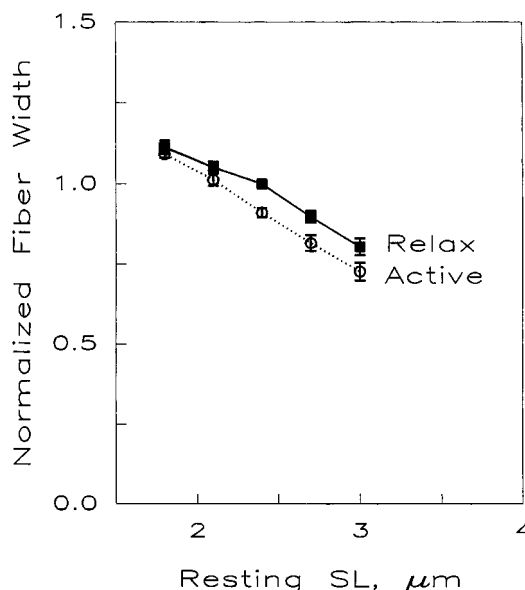

FIGURE 5   Average fiber width is plotted against SL during relaxation and activation. Data were first normalized to the width of relaxed fibers at SL $= 2.4$ μm. Then average was performed and plotted with SE. $n = 11$ (SL $= 1.8$ μm), 9 (2.1 μm), 28 (2.4 μm), 13 (2.7 μm), and 12 (3.0 μm).
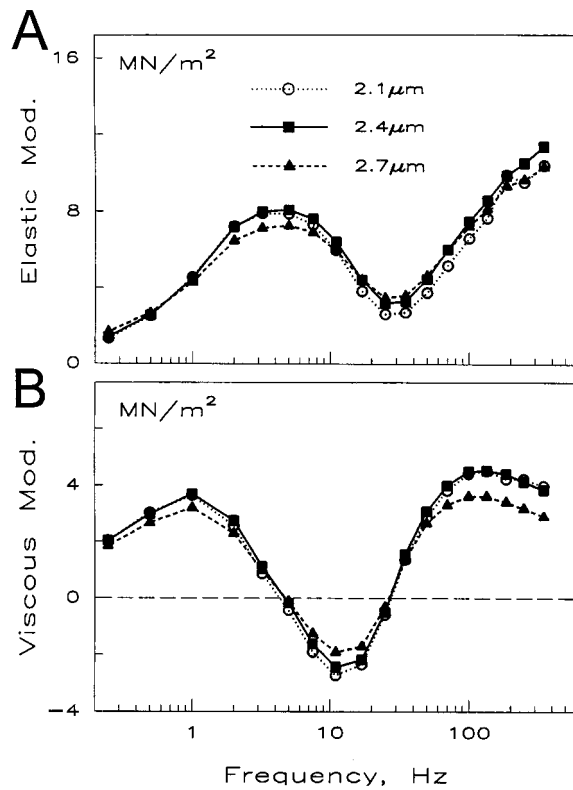
FIGURE 6   Elastic modulus in *A* and viscous modulus in *B* as functions of frequency at SLs of 2.1 μm ($n = 14$), 2.4 μm ($n = 14$), and 2.7 μm ($n = 5$). Frequencies (in Hz) used are 0.25, 0.5, 1, 2, 3.2, 5, 7.5, 11, 17, 25, 35, 50, 70, 100, 135, 187, 250, and 350.
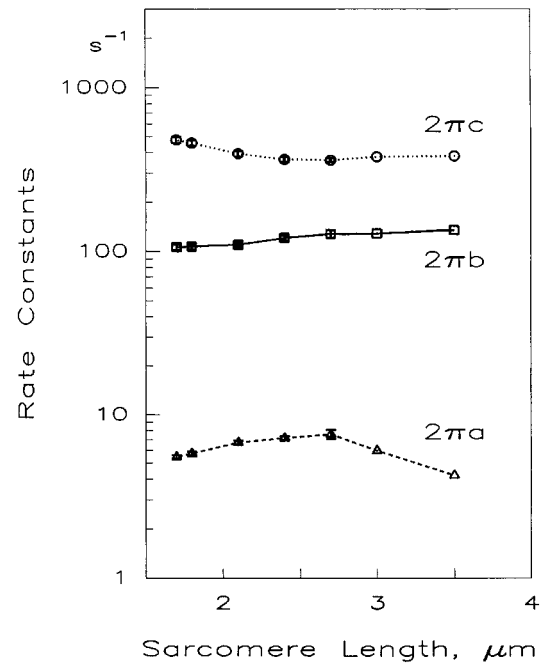

FIGURE 7   The apparent rate constants $2\pi a$, $2\pi b$, and $2\pi c$ were measured during the control activation, averaged, and plotted as the function of the sarcomere length. Error bars ($\pm$ SE) are entered but they are generally smaller than the plotting symbol size ($\pm$ 7%). There were 16 observations at SL = 1.7–2.4 μm, 6 at 2.7 μm, and 1 at 3.0–3.5 μm).

The elastic modulus represents elasticity of the preparation. Its value during maximal activation is small at low frequency and large at high frequency (Fig. 6 *A*). It has a local maximum at ~5 Hz and a local minimum at ~30 Hz. The viscous modulus represents the amount of work absorbed by the muscle in one cycle of length oscillation, and its value is small at both low and high frequencies (Fig. 6 *B*). The viscous modulus has two local positive peaks at ~1 Hz (= *a*) and ~100 Hz (= *c*) and one local negative peak at ~10 Hz (= *b*). These respectively correspond to the muscle's work absorption (processes A and C) and work generation (process B). The position of these three peaks does not change when SL is changed in the range of 2.1–2.7 μm (Fig. 6). These results indicate that SL does not significantly affect the apparent rate constants $2\pi a$, $2\pi b$, and $2\pi c$.

The complex modulus data (both elastic and viscous moduli) were fitted to Eq. 2 and the apparent rate constants were determined and plotted as the function of SL in Fig. 7. This figure shows that the rate constant $2\pi a$ increased (13 $\pm$ 7%, $\pm$ SE) when SL was increased from 2.1 μm to 2.7 μm but decreased toward higher and lower SL. The rate constant $2\pi b$ increased (16 $\pm$ 6%) when SL was increased from 2.1 μm to 2.7 μm but it did not change much over a larger SL range. The rate constant $2\pi c$ decreased (9 $\pm$ 4%) when SL was increased from 2.1 μm to 2.7 μm.

To demonstrate that compliance really increases as the SL is changed from 2.1 to 2.4 μm, we brought the muscle

fibers into the high-rigor state (Kawai and Brandt, 1976), and measured rigor tension and stiffness at 100 Hz. Rigor stiffness is a weak function of frequency and the choice of frequency is immaterial (Kawai and Brandt, 1980). The fibers were first activated by the control-activating solution and the high-rigor state was then induced by two washes with the rigor-2 solution. Fig. 8 *A* shows rigor tension plotted against SL and Fig. 8 *B* shows stiffness plotted against SL. Both sets of the data were normalized to the value at SL = 2.4 μm and averaging was then performed. Fig. 8 *C* shows the ratio of tension to stiffness in %L_0. From these data we conclude that rigor tension was the same when SL was changed from 2.1 μm to 2.4 μm (Fig. 8 *A*), whereas rigor stiffness decreased (compliance increased) for the same SL change. The increase in compliance (= 1/stiffness) is also seen in Fig. 9 *C*. From the normalized stiffness data (1.223 $\pm$ 0.030) at SL = 2.1 μm in Fig. 9 *B* and the model of Figs. 1 and 9, we deduced that thin filament (I-band) compliance is 35 $\pm$ 3% of sarcomere compliance when SL is 2.4 μm, and that it is 24 $\pm$ 2% when SL is 2.1 μm.

DISCUSSION

The effect of thin filament compliance

The purpose of the present study was to examine whether thin-filament compliance affects our ability to measure the rate constants that characterize the cross-bridge kinetics. We
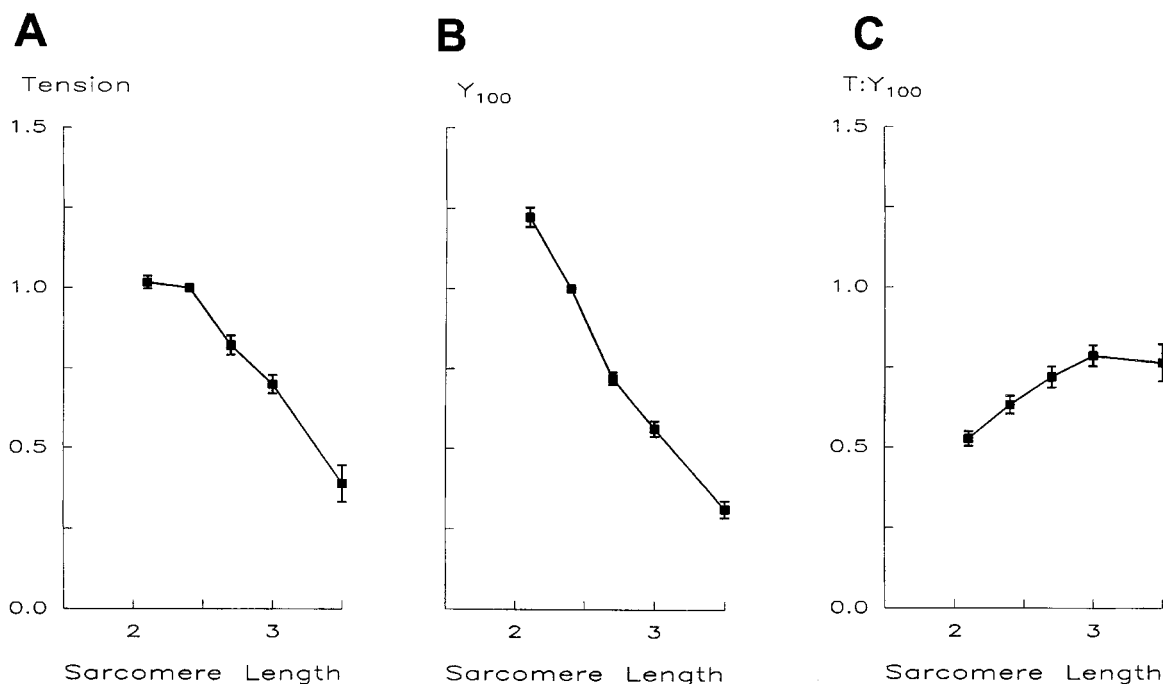
A
Tension

B
Y_{100}

C
$T:Y_{100}$

FIGURE 8   Rigor tension is plotted in *A*, rigor stiffness at 100 Hz (Y_{100}) in *B*, and the tension-to-stiffness ratio ($T:Y_{100}$) in *C*. The rigor was induced with the rigor-2 solution following to control activation. SL is shown in abscissa in micrometers. Resting tension and stiffness were measured before activation and subtracted from corresponding values during rigor induction. In *A* and *B*, the data are normalized to the value at SL = 2.4 μm. The unit of *C* is %L_0, where L_0 is the fiber length at SL = 2.4 μm. An average of 10 experiments is shown with SE.

S.L.

A   1.8μm

B   2.1μm

C   2.4μm

D   2.7μm

FIGURE 9   Projected sarcomere structure of rabbit psoas fibers based on thin filament length (1.12 μm), thick filament length (1.63 μm), and bare zone (0.16 μm).

aimed at comparing the rate constants at two different SLs in which the length of overlap between thick and thin filaments is the same, but one (SL = 2.4 μm) has a longer I-band than the other (SL = 2.1 μm), causing extra in-series compliance (Higuchi et al., 1995). The sarcomere structure is based on the filament lengths, as depicted in Fig. 9 and summarized by Higuchi et al. (1995). Here we assume that the extra thin filament in the middle of the sarcomere (bare zone) does not play a role in cross-bridge kinetics because there are no cross-bridges to interact in the bare zone. Owing to some sarcomere shortening during activation (Fig. 3), a fair comparison can be made between the starting (resting) SL of 2.1 μm and 2.7 μm. On average, SL 2.1 μm shortened to 2.0 μm, and SL 2.7 μm to 2.5 μm, during control activation (Fig. 3). We did not use the data from shorter SL for comparison because isometric tension declines significantly (Fig. 4), perhaps caused by cross-bridges interacting with the thin filaments of wrong polarity. Such interaction would have resulted in an altered cross-bridge kinetics, as evidenced by larger $2\pi c$ and smaller $2\pi a$ (Fig. 7).

The series compliance *q*, which is due to the thin filament, is directly proportional to the width of the I-band. In Fig. 9 *B* (SL = 2.1 μm) the width of the half I-band is 0.225 μm and in Fig. 9 *C* (SL = 2.4 μm) it is 0.385 μm. Thus, *q* decreases to 58% (= 0.255/0.385) when SL is decreased from 2.4 to 2.1 μm. This projected decrease in compliance is actually seen as an increase in stiffness in Fig. 8 *B*, and a decrease in the tension-to-stiffness ratio (Fig. 8 *C*). Because compliance of the cross-bridges (1/*k*) and that of the thin filament (*q*) are comparable at SL $\sim$ 2.4 μm (Wakabayashi et al., 1994), *kq* $\sim$ 1. From Eq. 1, we then calculate that the apparent rate constant should decrease by 21% when SL is increased from 2.1 to 2.4 μm. Similarly, the compliance model proposed by Luo et al. (1993) shows a reduction of the apparent rate constant by 20–25% (their Fig. 3B). However, these predictions are not supported by our data. In Fig.
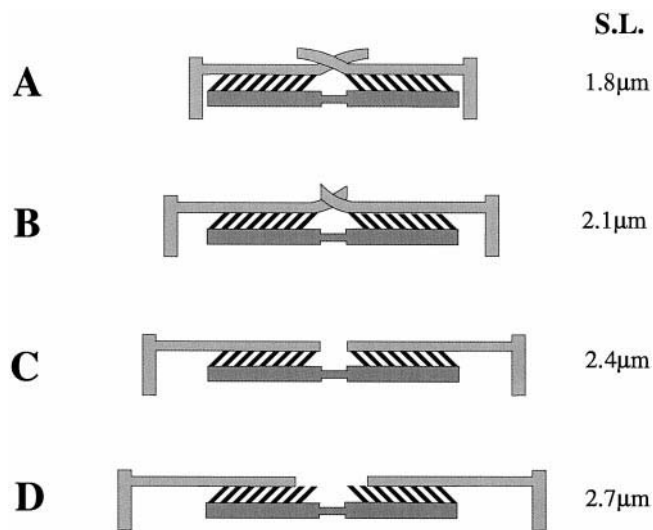
7, we find that $2\pi a$ increases $13 \pm 7\%$ ($\pm$ SE), $2\pi b$ increases $16 \pm 6\%$, and $2\pi c$ decreases $9 \pm 4\%$ as SL is changed from 2.0 to 2.5 μm. Thus, our results on $2\pi a$ and $2\pi b$ are opposite from those anticipated based on series compliance, and our result on $2\pi c$ (9% decrease) is not as much as anticipated (21% decrease) based on series compliance. The slight reduction in $2\pi c$ can be explained by compression of the lattice spacing (see below). The range of SL (2.0–2.5 μm) we studied includes the range (2.1–2.4 μm) to demonstrate the effect of extra series compliance and the effect is unidirectional, hence the effect would be smaller for the SL range 2.1–2.4 μm. From these results, we infer that the rate constants measured with sinusoidal analysis under our experimental conditions are not affected by the series compliance in the way expected from model analysis.

Change in the lattice spacing

When SL is increased, the lattice spacing of thick and thin filaments decreases, which may in turn alter the cross-bridge kinetics. Fig. 5 demonstrates that the fiber width is diminished by 10% when SL is increased from 2.1 to 2.4 μm, and another 10% when SL is further increased from 2.4 to 2.7 μm. We demonstrated earlier by using equatorial x-ray diffraction that the fiber width and the lattice spacing are proportionally related (Kawai et al., 1993) and that a 10% reduction in the fiber width occurred when ~4% of Dextran T-500 was introduced to the activating solution (Zhao and Kawai, 1993). When 4% Dextran T-500 was introduced, $2\pi a$ decreased by 2%, $2\pi b$ decreased by 10%, and $2\pi c$ decreased by 7% under similar experimental conditions (Fig. 6a in Kawai and Schulman, 1985). Thus, if the effect of the change in the lattice spacing is subtracted, then the effect of SL would be a $15 \pm 7\%$ increase on the rate constant $2\pi a$, a $26 \pm 6\%$ increase on $2\pi b$, and a $2 \pm 4\%$ decrease on $2\pi c$. In other words, when the lattice spacing change is subtracted, we cannot detect any indication of a decrease in any of three apparent rate constants.

Cross-bridge models with series compliance

The question arises, why does the series compliance not diminish the apparent rate constants? A model proposed by Luo et al. (1993), who introduced series compliance into the model of A. F. Huxley (1957), predicts that the series compliance diminishes the rate constant by 20–25%. The rate constant they discussed ranges from 4 to 66 s^{-1}, which is between our apparent rate constants $2\pi a$ and $2\pi b$. We found that both $2\pi a$ and $2\pi b$ increased as SL is increased from 2.1 to 2.7 μm (Fig. 7). Similarly, our analysis using equivalent mechanical arrangement (Fig. 1) predicts that the series compliance diminishes the rate constants by 21% according to Eq. 1. These models are based on the assumption that cross-bridge compliance is similar to that of filaments, primarily based on x-ray diffraction studies compar-

ing relaxed and rigor conditions (Huxley et al., 1994; Wakabayashi et al., 1994). It is possible that these conditions may not apply to our experimental conditions.

One possibility is that the fraction of cross-bridges strongly attached to the thin filament during the control activation may not be as large as previously thought. Recent evidence that considers series compliance on tetanically stimulated frog tibialis anterior fibers reported that the fraction of attached cross-bridges is 43% or less (Linari et al., 1998). Other experiments using a spin probe attached to the myosin head showed a value of 20–30% (Cooke et al., 1982; Ostrap et al., 1995). If this is the case, then stiffness associated with the overlap region becomes smaller, hence compliance of the overlap region becomes larger. The fraction of attached cross-bridges also changes depending on the activating conditions; most notably, the fraction increases with temperature (Zhao and Kawai, 1994b) and it decreases with phosphate (Kawai and Halvorson, 1991). If the fraction of attached cross-bridges is 40%, then the anticipated decrease in the rate constant is 9% instead of 21% (Eq. 1). Because we detected an increase of rigor compliance when SL is changed from 2.1 μm to 2.4 μm although the rate constants $2\pi a$ and $2\pi b$ are not decreased, there is a good possibility that compliance of the overlap zone is significantly large during full activation.

The second possibility is that thin filament compliance may not be as large as that of cross-bridges. Based on the data obtained during rigor induction (Fig. 8), we deduced that the thin filament compliance is 24% of sarcomere compliance at SL = 2.1 μm and that the compliance increases to 35% at SL = 2.4 μm, both during rigor induction. If this fact is taken into account together with the fact that the fraction of attached cross-bridges during control activation may be 40% of the rigor state, then the effect on the rate constant would be 8% reduction when SL is increased from 2.1 to 2.4 μm. We found no evidence of this decrease in the rate constant $2\pi a$ or $2\pi b$. The 9% decrease in the rate constant $2\pi c$ can be interpreted by the shrinkage of the lattice spacing (above).

The third possibility is that the series compliance may have two components, one originating from the thin filament and the other from attached ends. The hypothesis here is that the compliance of the thin filament may increase with SL but the end compliance may decrease, with the net effect of decreasing series compliance as the SL is increased from 2.1 μm to 2.4 μm. Although this hypothesis is consistent with $2\pi a$ and $2\pi b$ in Fig. 7, it is not consistent with the stiffness data of Fig. 8 *B*: we did detect an increase in compliance as the SL was increased. Thus we rule out the possibility of two antagonizing sources of compliance.

In contrast to the rate constant results, isometric tension diminishes significantly (45%) at short SL (1.7 μm) (Fig. 4). This observation is presumably related to the fact that cross-bridges interact with the thin filament of wrong polarity at the center of a sarcomere and as depicted in Fig. 9 *A*.

Comparison to other works

Edman (1979) demonstrated that maximum unloaded shortening velocity (V_{max}) is not affected by SL in the range 1.7–2.7 μm in intact frog semitendinosus fibers. A similar result was reported by Edman (1988) in frog anterior tibialis muscle fibers in the SL range 1.85–2.60 μm, except that an additional parameter, *a*, was slightly affected by SL. Although these results appear comparable to our results with the rate constants changing little in the SL range 1.7–3.5 μm (Fig. 7), the experimental conditions are somewhat different. Hence, such comparison should be made with caution: the V_{max} measurements were carried out under the unloaded condition in which the number of attached cross-bridges are presumably minimized, whereas our experiments were carried out near or at the isometric condition in which the number of attached cross-bridges are presumably maximized. McDonald et al. (1997) reported that the rate constant (k_{tr}) of tension recovery increased significantly when SL was increased from 2.0 to 2.3 μm in rat slow-twitch and rabbit fast-twitch skeletal muscle fibers. However, this experiment was carried out when a large length change ($\sim$8%) was applied, so a direct comparison with our experiments may not be possible.

CONCLUSION

We have demonstrated that the rate constants we detect using sinusoidal analysis are not significantly influenced by the introduction of series compliance under our experimental conditions.

REFERENCES

Bagni, M. A., G. Cecchi, F. Colomo, and C. Poggesi. 1990. Tension and stiffness of frog muscle fibres at full filament overlap. *J. Muscle Res. Cell Mot.* 11:371–377.

Cooke, R., M. S. Crowder, and D. D. Thomas. 1982. Orientation of spin labels attached to cross-bridges in contracting muscle fibres. *Nature.* 300:776–778.

Dantzig, J., Y. Goldman, N. C. Millar, J. Lacktis, and E. Homsher. 1992. Reversal of the cross-bridge force-generating transition by the photogeneration of phosphate in rabbit psoas muscle fibers. *J. Physiol.* 451: 247–278.

Edman, K. A. P. 1979. The velocity of unloaded shortening and its relation to sarcomere length and isometric force in vertebrate muscle fibres. *J. Physiol.* 291:143–159.

Edman, K. A. P. 1988. Double-hyperbolic force-velocity relation in frog muscle fibres. *J. Physiol.* 404:301–321.

Fortune N. S., M. A. Geeves, and K. W. Ranatunga. 1991. Tension responses to rapid pressure release in glycerinated rabbit muscle fibers. *Proc. Natl. Acad. Sci. USA.* 88:7323–7327.

Higuchi, H., T. Yanagida, and Y. E. Goldman. 1995. Compliance of thin filaments in skinned fibers of rabbit skeletal muscle. *Biophys. J.* 69: 1000–1010.

Huxley, A. F. 1957. Muscle structure and theories of contraction. *Prog. Biophys. Chem.* 7:255–318.

Huxley, A. F., and R. M. Simmons. 1971. Proposed mechanism of force generation in striated muscle. *Nature.* 233:533–538.

Huxley, H. E., A. Stewart, H. Sosa, and T. Irving. 1994. X-ray diffraction measurements of the extensibility of actin and myosin filaments in contracting muscle. *Biophys. J.* 67:2411–2421.

Kawai, M., and P. W. Brandt. 1976. Two rigor states in skinned crayfish single muscle fibers. *J. Gen. Physiol.* 68:267–280.

Kawai, M., and P. W. Brandt. 1980. Sinusoidal analysis: a high resolution method for correlating biochemical reactions with physiological processes in activated skeletal muscles of rabbit, frog and crayfish. *J. Muscle Res. Cell Motil.* 1:279–303.

Kawai, M., and M. I. Schulman. 1985. Cross-bridge kinetics in chemically skinned rabbit psoas fibres when the actin-myosin lattice spacing is altered by dextran T-500. *J. Muscle Res. Cell Mot.* 6:313–332.

Kawai, M., and H. R. Halvorson. 1989. Role of MgATP and MgADP in the crossbridge kinetics in chemically skinned rabbit psoas fibers. Study of a fast exponential process (C). *Biophys. J.* 55:595–603.

Kawai, M., and H. R. Halvorson. 1991. Two step mechanism of phosphate release and the mechanism of force generation in chemically skinned rabbit psoas muscle. *Biophys. J.* 59:329–342.

Kawai, M., J. S. Wray, and Y. Zhao. 1993. The effect of the lattice spacing change on cross-bridge kinetics in chemically skinned rabbit psoas muscle fibers. I. Proportionality between the lattice spacing and the fiber width. *Biophys. J.* 64:187–196.

Linari, M., I. Dobbie, M. Reconditi, N. Koubassova, M. Irving, G. Piazzesi, and V. Lombardi. 1998. The stiffness of skeletal muscle in isometric contraction and rigor: the fraction of myosin heads bound to actin. *Biophys. J.* 74:2459–2473.

Luo, Y., R. Cooke, and E. Pate. 1993. A model of stress relaxation in cross-bridge systems: effect of a series elastic element. *Am. J. Physiol.* 265:C279–C288.

McDonald, K. S., M. R. Wolff, and R. L. Moss. 1997. Sarcomere length dependence of the rate of tension redevelopment and submaximal tension in rat and rabbit skinned skeletal muscle fibres. *J. Physiol.* 501.3: 607–621.

Ostrap, E. M., V. A. Barnett, and D. D. Thomas. 1995. Resolution of three structural states of spin-labeled myosin in contracting muscle. *Biophys. J.* 69:177–188.

Ranatunga, K. W. 1996. Endothermic force generation in fast and slow mammalian (rabbit) muscle fibers. *Biophys. J.* 71:1905–1913.

Stephenson, D. G., and D. A. Williams. 1982. Effects of sarcomere length on the force-pCa relation in fast- and slow-twitch skinned muscle fibres from the rat. *J. Physiol.* 333:637–653.

Wakabayashi, K., Y. Sugimoto, H. Tanaka, Y. Ueno, Y. Takezawa, and Y. Amemiya. 1994. X-ray diffraction evidence for the extensibility of actin and myosin filaments during muscle contraction. *Biophys. J.* 67: 2422–2435.

Wang, G., and M. Kawai. 1996. Effects of MgATP and MgADP on the cross-bridge kinetics of rabbit soleus slow-twitch muscle fibers. *Biophys. J.* 71:1450–1461.

Wang, G., and M. Kawai. 1997. Effects of in-series thin filament compliance on the elementary steps of the cross-bridge cycle in skinned rabbit psoas muscle fibers. *Biophys. J.* 72:A281 (Abstr.)

Zhao, Y., and M. Kawai. 1993. The effect of the lattice spacing change on cross-bridge kinetics in chemically skinned rabbit psoas muscle fibers. II. Elementary steps affected by the spacing change. *Biophys. J.* 64: 197–210.

Zhao, Y., and M. Kawai. 1994a. BDM affects nucleotide binding and force generation steps of cross-bridge cycle in rabbit psoas muscle fibers. *Am. J. Physiol.* 266 (*Cell Physiol.* 35):C437–C447.

Zhao, Y., and M. Kawai. 1994b. Kinetic and thermodynamic studies of the cross-bridge cycle in rabbit psoas muscle fibers. *Biophys. J.* 67: 1655–1668.

Zhao, Y., P. M. G. Swamy, K. A. Humphries, and M. Kawai. 1996. The effect of partial extraction of troponin C on the elementary steps of the cross-bridge cycle in rabbit psoas muscle fibers. *Biophys. J.* 71: 2759–2773.